Authors Response to Referee Comments

Reviewer #1 (W. Eugster)

Comment 1: Abstract
For me as a reader the keyword would have been "thermokarst", but this does not appear in the abstract. I wonder why – it is nicely introduced in the Introduction, but I definitely would argue that looking at a retrogressive thaw slump is one form of thermokarst and should definitely be put in context already in the Abstract.
The "increase in frequency and magnitude" (line 5/19782) is never substantiated in the text (or I did not find it). The information I could find is the 0.4% of area given as a personal communication on line 1/19798. This is not sufficent to prominently place the "increase in frequency and magnitude", so please either substantiate this in the text or remove this from the abstract. It is important that we do not sell expectations as facts in scientific papers.
Rounding the numbers: on lines 13/14 you give the uptake as 3.84 gC/m2 and 12.48 gC/m2, which means ±0.01 gC/m2. This accuracy is unrealistic, so please round to 1 decimal (or provide some evidence that the uncertainty is really as good as ±0.01 gC/m2).

Responses:

➔ We have altered the abstract text to include the term thermokarst (line 27) as follows "*Thermokarst and permafrost disturbances, especially active layer detachments and retrogressive thaw slumps, are present across the Fosheim Peninsula, Ellesmere Island, Canada.*" We have also included the keyword thermokarst in the introduction (lines 76-79): "*These disturbances are usually linked to thermokarst and affect soil temperature, water quality and soil nutrients (Mackay, 1970, Lamoureux and Lafrenière, 2009, Lantz et al., 2009, Kokelj and Lewkowicz, 1998, Kokelj and Lewkowicz, 1999).*"

➔ The increase in frequency and magnitude refers to multiple publications (Lewkowicz, 1990; Lewkowicz and Harris, 2005) analyzing permafrost disturbances on the Fosheim Peninsula (line 589-592). We now mention this in the discussion: "*The frequency and magnitude of these land surface disturbances appear to be increasing across the Fosheim Peninsula (and elsewhere in the Arctic) as a result of the warming climate, thus exacerbating these impacts (Lewkowicz, 1990; Lewkowicz and Harris, 2005b; Lantz and Kokelj, 2008).*" In addition, one of the authors (GHRH) has observed a substantial increase in the frequency and magnitude of disturbance since the early 1990s in this study area. This has been confirmed by WH Pollard, who visits this region annually (pers. comm., 2014).

➔ Values have been rounded to 3.8 g C m^{-2} and 12.5 g C m^{-2} (line 36) (over the measurement period).

Comment 2: Units
You present EC fluxes in gC/m2, but chamber fluxes in μmol/m2/s. This is confusing,

since the physical principle behind the measurements is the same if you use optical absorption spectroscopy: you measure the absorption of light which is proportional to µmol/m3, and then convert to e.g. a mass flux. My suggestion (since at the end we expect that the two fluxes should be comparable): homogenise the reporting to either report mass fluxes or mole fluxes, but not a mixture of both.

Response: When individual (e.g. hourly) values are compared (as in Figure 6), we use µmol m^{-2} s^{-1}. However, to summarize our EC measurements over the entire season (and component periods), we chose g C m^{-2} day^{-1}. This has been consistently applied across the manuscript and is commonly done in the literature.

Comment 3: References
I am not really into retrogressive thaw slumps, but what surprises me is that none of the effects on the aquatic systems is mentioned. Please have a look at the literature below that I extraced from the Toolik LTER publication database (without reading everything in detail) and consider whether this is not also an aspect to mention at your site: how the thaw slump and export of the silty material downriver may affect the aquatic ecosystems.

Response: We now mention the hydrologic impacts (on downstream water quality) of these systems as studied in the Canadian High Arctic in the introduction (lines 76-79) and in the discussion (lines 585-589). As our site is within the High Arctic, we added references that are located within this region.
In the introduction, we state "*These disturbances are usually linked to thermokarst and affect soil temperature, water quality and soil nutrients (Mackay, 1970, Lamoureux and Lafrenière, 2009, Lantz et al., 2009, Kokelj and Lewkowicz, 1998, Kokelj and Lewkowicz, 1999)*".
In the discussion, we mention "*Although the landscape area directly impacted by disturbance at this time is minimal, indirect impacts such as the lateral export of dissolved and particulate organic matter (hence, carbon) through streams and the hydrologic network are also important (Lamoureux and Lafrenière, 2009, Kokelj and Lewkowicz, 1998, Kokelj and Lewkowicz, 1999).*"

Comment 4: Annual effects
At the end of the discussion (lines 3–13/19799) you quickly scratch the surface of longer-term fluxes. Given that you have only 32 days of measurements it does not appear to be defensible to relate this to longer term effects, rather consider this a case study and remove that paragraph. Maybe lines 3–8 can be kept (but then it would be good to know more about "logistic constraints" – a typical constraint is that you want to go on vacation and hence don't have the time to continue measuring, but it could also be something that is more informative to the reader; maybe you want to say that the systems could not have been left alone due to the activity of the RTS, and hence you ran out of personel funding to service the site? Maybe there is a justification to say that one learns most during that part of the season and not during the later part of the season anyway?).

Response:
➔ We have added in details regarding the site logistics (lines 618-621): "*Due to

the dynamic nature of these disturbances, the site could not be left alone as personnel were needed monitor the slide edge location and adjust the equipment as needed. Leaving the site unmanned would have put the equipment at risk."
We mention the annual trends found at other Arctic sites while acknowledging the limitations of our study (lines 621-630), as periods outside of our measurement period may also be important, and could be explored in future studies.

Comment 5: Appendix
I find an appendix that only has 10 lines of text rather special. The aspect covered in the appendix is a component covered by the text and relevant to the story, so it is not really an appendix. Why not include that paragraph into material and methods? The style is different and needs some change though, but depending on what other reviewers say I would definitely include Fig. A1 as a normal figure into the manuscript.

> Response: Thank you for this suggestion. We have followed the suggestion and incorporated the Appendix material into the manuscript.

DETAILS
19783/7–8: this sentence does not sound right to me, like lacking the main verb: "Current estimates are likely an underestimation, by as much as a factor of two, due to difficulties measuring and uncertainty regarding carbon storage in cryoturbated soils".

> Response: This sentence (lines 64-67) has been reworded as follows
> "*Measurement difficulties and uncertainty regarding carbon storage in cryoturbated soils may result in an underestimation of current estimates, by as much as a factor of two (Hugelius et al., 2013).*"

19784/13: maybe the Mbufong et al. (2014) paper has a relation to this aspect.

> Response: Thank you for this reference. We have incorporated these findings (lines 104-105) into this paragraph as follows: "*Variability may be explained by nutrient availability, substrate quantity and soil organic matter (Mbufong et al., 2014).*"

19786/5–8: this is not quite correct; please double-check with Eugster et al. (2005), but I think the implicit assumption you make here is not the 24 h of sunlight but that in your case (high Arctic) the sun is relatively high above the horizon even at midnight, were in the low Arctic where we measured, the conditions at night are still more night-time like despite the sun being above the horizon. I think a more clear rephrasing will help the readers who are not familiar with the differences between high Arctic and low Arctic conditions.

> Response: This section has been modified to reflect the light conditions over 24 hour daylight as follows (lines 125-128)
> ➔ "*Further, with 24 hours of daylight during which the sun remains relatively high above the horizon, the usual partitioning methods for EC measurements into component fluxes (Reichstein et al., 2012) are not applicable, as they rely on nighttime measurements, or measurement during low light conditions.*"

19789/14: I think that the correct term would rather be "partition" or "unmix" than "isolate". Moreover, I am not clear what you mean with "pure fluxes". Maybe component fluxes?

Response: We have replaced "isolate" with "partition" and "pure fluxes" with "component fluxes" (lines 246-248). This sentence now reads:
➔ "*By solving a set of linear equations (Eq. 3 and Eq. 4), we are able to partition the component fluxes of CO_2 (Fig. 2) from the disturbed tundra (NEE$_d$) and from the undisturbed tundra (NEE$_c$) from both towers (T1 and T2)*"

19790/16: how exactly did you define "soil surface", namely when mosses were present?

Response: Soil surface was defined as the ground surface in any border of the collar, which was installed for level conditions across the site.
We have inserted the following sentence (lines 286-287): "*As moss cover was minimal and discontinuous, the location of the ground surface could be easily identified as the upper surface of the soil.*"

19790/24: there are still two types of non-steady state chambers: vented ones and unvented ones. Can you be more specific which kind you used?

Response: We used a vented non-steady state chamber, and text has been updated (lines 295-296) to reflect this system as follows: "*A non-steady state vented portable chamber system similar to Jassal et al.(2005) was used to measure fluxes from each collar using transparent and opaque chambers.*"

19791/20: not considering the humidity effects leads to substantial overestimation of photosyntheses, see Pérez-Priego et al. (2015). Why did you not correct for humidity effects? Is there an argument to not do it?

Response: We have corrected for humidity. The manuscript has been updated with corrected values throughout.

19791/26: this is backwards! Why not write GPP = Re – NEE which looks more straight forward to the reader?

Response: The equation was rewritten as suggested.

19793/23: over which period were the 21 m/s determined? Raw 20 Hz spike, or e.g. a 30-min average?

Response: The maximum wind speed was determined from the raw 20 Hz spike, which is now reflected in the text (lines 395-397) as follows: "*There was a significant windstorm beginning on 22 July and that lasted 24 hours, with wind speeds (as determined from the raw 20 Hz spikes) of up to 21 m s^{-1}.*"

19794/19: rounding to 1 decimal seems more appropriate

Response: We have rounded to 1 decimal place.

19794/21: Fig. 4 does not show any correlation. Even the comparison between Fig. 4 and Fig. 3 does not allow for the assessment of correlations (this would be unpaired sample comparison, whereas correlation assumes paired samples). So either remove the reference to Fig. 4 or add a graph showing the correlation.

Response: We have removed the reference to Fig. 4.

Fig. 1: if the view is really towards SW, then this valley rather looks like running in WSW–ENE direction. Please double-check (the Google Earth images are not good enough to allow to see this at the coordinates you specify for the site).

Response: Thank you for spotting this error. Orientation of the photo has been checked and corrected. The view is towards the south and the caption has been updated accordingly.

Fig. 6: can you add uncertainty bars to the chamber flux measuremens? Also for the EC measurements some indication on the uncertainty (either bars of symbol size) would allow for a more critical visual assessment by the reader.

Response: We have decided not to include uncertainty bars on Fig. 7 as we felt it would overwhelm the plot. Error associated with the data measured using the chamber system can be found in Fig. 8 and Table 2. We have added error bars to Fig. 6 and this information can also be found in Table 1.

Anonymous Referee #2

Comment
This is a well thought out and executed study, and well written. However, I'm a bit concerned about the actual eddy covariance NEP data because the authors used LICOR 7500 open path CO_2 sensors. As far as I can tell, no attempt was made to correct for the well-documented heating issues that these open path 7500 sensors have, espe- cially in places where temperatures are cold (i.e., their site). The heating issues result in exaggerated CO_2 uptake rates, which can be particularly important in regions where NEP is already extremely low. There are publications that advice how to best deal with this issue (e.g., Burba GG, McDermitt DK, Grelle A, Anderson DJ, Xu L (2008) Addressing the influence of instrument surface heat exchange on the measurements of CO_2 flux from open-path gas analyzers. Global Change Biology, 14, 1854–1876). Can the authors please address this prior to the final publication of this article. It's very important!

Response: Thank you for this valuable comment – we acknowledge that under cold conditions instrument surface heat may critically affect the ability to measure CO_2

fluxes with an open-path sensor, in particular with an upright mounted sensor (Burba et al., 2008). The EddyPro® manual summarizes "When CO_2 and H_2O molar densities are measured with the LI-7500 in cold environments (low temperatures <u>below -10 °C</u>), a correction should be applied to account for the additional instrument-related sensible heat flux, due to instrument surface heating/cooling."
(<u>https://www.licor.com/env/help/eddypro6/Content/Calculating_Off-season_Uptake_Correction.html</u>).

We did not apply this correction because it would lead to unrealistic values ('overcorrection') for the following three reasons:

- Our measurements were made during July, with 24 hour sunlight. Our <u>average air temperature was +10ºC</u>. Temperatures never dropped below 2°C, and reached as high as 16°C. Hence, ambient temperatures did not fall within the critical range of < -10ºC, where fluxes are affected, mentioned in Burba et al. (2010).
- In addition, our sensors (Li-7500) were <u>mounted at an angle of 30º to minimize issues associated with this heating</u> and reduce pooling of moisture on the windows. The correction cannot be employed with a tilted sensor. Burba et al. (2008) note that the correction "… assumes that the instrument is mounted in a near-vertical orientation". Previous work by our colleague Prof. A. Black (UBC, pers. comm.) has shown that a tilted sensor does not cause measurement differences between open-path and closed-path systems. A comparison between fluxes measured with a tilted Li-7500 sensor and a closed path system as function of temperature can be found in the appendix to this response.
- In our current approach (i.e. without correction) <u>closed chamber measurements and the EC approach match well</u> (RMSE = 0.6 µmol m^{-2} s^{-1}). If we would correct fluxes according to Burba et al. (2008) and assume the sensor was mounted upright, we found that the correlation between chamber measurements and EC measurements becomes worse (RMSE = 1.4 µmol m^{-2} s^{-1}). To us, this is a strong argument that the correction would be incorrectly applied (assuming a vertically mounted sensor) and would not improve our dataset.

Additional supporting evidence

Demonstration that a tilted sensor mounting of the Li-7500 sensor causes no sensor disagreement to a closed-path system between 2ºC and 16ºC.

To investigate whether there are any systematical differences between measuring CO_2 fluxes with a tilted open-path (OP, Li-7500) vs. a closed-path (CP) analyzer in the range of the currently observed temperatures, we used a dataset sampled by the UBC Biometeorology group (Prof. A. Black, pers. comm.) and provided to us. This dataset was recorded a forest clear-cut in Saskatchewan, Canada (Fluxnet site HJP02, Zha et al. 2009, Figure 1) at a comparable height to our systems. We used data from June – December 2004 when both a Li-7500 open path analyzer tilted by about 30º (same tilt we used in our measurements) and a closed path

analyzer (Li-7000, Fluxnet Canada standard) were operated simultaneously. Air temperatures during this time covered the range from -15 to +20ºC.

Figure 1: Tilted open-path and inlet for closed-path system at the HJP02 Fluxnet Canada site (Photo by Zoran Nesic, UBC)

The half-hourly differences between F_{CO_2} measured by the tilted OP and F_{CO_2} measured by the CP were binned by air temperature (2 K bins). Figure 2 shows that for the range between 0 and 20ºC, the systems are not systematically different, while below 0ºC the OP instrument starts to systematically underestimate fluxes, which indeed becomes a major issue < -10ºC - presumably due to the sensor heating effect. Temperatures during our measurements for the current study in the High Arctic were always between 2ºC and 16ºC, with an average of 10ºC, so we do not expect that our fluxes were compromised with a tilted sensor mounting of the Li-7500.
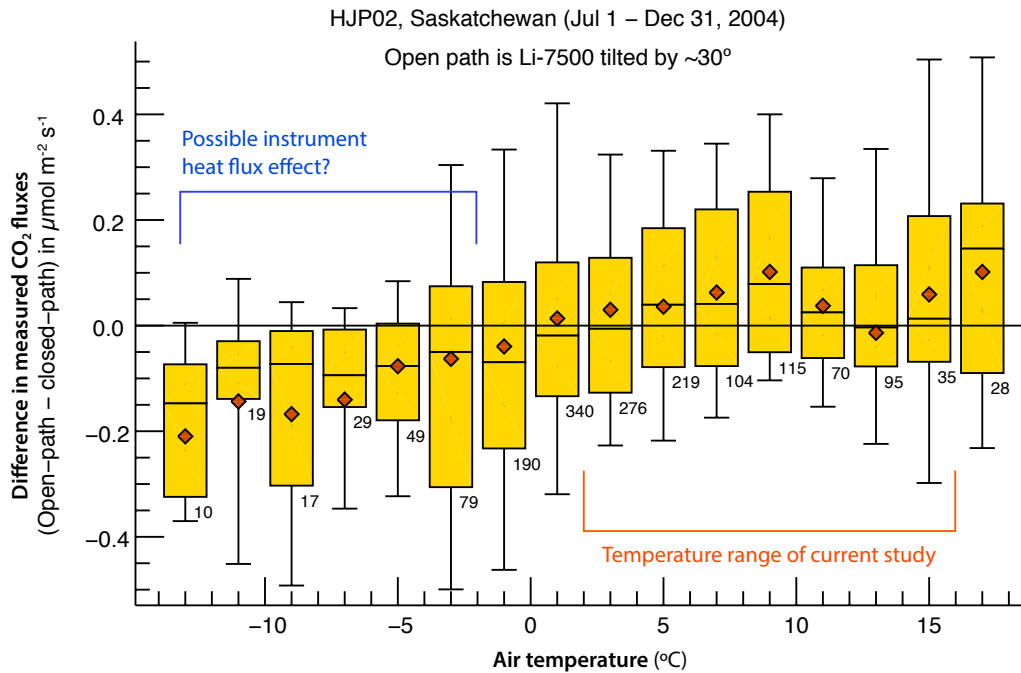
Figure 2: Difference between CO_2 fluxes determined by open path and closed-path system from July 1, to December 31, 2004 at the Canada Fluxnet Site HJP02. Diamonds are mean values in each bin, the boxes cover the 25% and 75% percentiles, with the horizontal bar being the median. The whiskers show the 5 and 95% percentiles. Numbers are the number of half hourly values in each bin (when both systems provided high quality data).

Anonymous Referee #3

Comment 1:
    I am little bit confused with the general structure of the introduction (particularly from line 90 to line 126), where some interesting things (e.g., the importance for NEE measurements or the influence of tundra vegetation) should be before detailing the objectives, whereas some information (such as the design developed in this study or the use of static chamber) should be placed in the materials and methods section. Also, it would be nice to know which mechanisms are proposed to hypothesize that RTS will impact the carbon balance (lines 80-82).

    Response: We have modified the introduction so that the objectives follow the introduction of the importance of measurements. The introduction section ends with "*In this study, we analyze the impacts of RTS on CO_2 exchange in a high Arctic tundra ecosystem. Our main research objective was to examine how growing season NEE and its component fluxes vary between a RTS and undisturbed tundra.*" (lines 132-134). We have moved details regarding the design of the EC system to the methods section (line 162-167): "*An appropriate sampling design was necessary to quantify the CO_2 fluxes between land surface and atmosphere simultaneously from disturbed and undisturbed sites in close proximity (Hollinger and Richardson, 2005). We used a dual eddy covariance approach, which was advantageous over a single eddy covariance tower as we were able to measure fluxes simultaneously from disturbed tundra and the surrounding undisturbed tundra (Fig. 1; Fig. 2).*"

Comment 2:
    Finally, is it possible to go further in the discussion to put into perspectives quantitative estimates of such landscape disturbance? I know that this is probably tough since the authors may not have good estimates of disturbance areas (just based on personal communication) and there are gaps for fall, winter, and spring seasons.

    Response: We have provided an estimate of landscape disturbance across the study location (personal communication: 585). As details of the rates of landscape change are minimal at this site, we have included an additional paper, which seeks to quantify permafrost disturbance across the Mackenzie Delta region of Canada, where increasing rates of thaw are discussed (Lantz and Kokelj, 2008). While not quantitative, one of the authors (GHRH) has seen the increased frequency and magnitude of these disturbances during nearly annual flights over the area and visits to sites on the Fosheim Peninsula since 1989. Other colleagues, in particular A. Lewkowicz and W. Pollard have also conducted permafrost research on the Fosheim Peninsula, and have told us they also clearly see an increase in these

disturbances since the late 1980s. Providing a robust estimate of the change in number and area of these disturbances would be an excellent research project.

We have addressed the following minor comments as follows:

Abstract
Line 29: Please precise the country (Canada)

Response: Canada has been added.

Introduction
Line 52: "ground", do you mean soil or top soil? Precise please.

Response: Line has been clarified to reflect organic carbon as follows: "*The northern permafrost zone carbon inventory estimates the quantity of organic carbon stored in the top 3m of frozen and unfrozen soils in northern circumpolar permafrost regions …*"

Line 80: Remove "(Lantz et al., 2009)"

Response: This reference has been removed.

Line 88: Use either "retrogressive thaw slump" or "RTS" in the text.

Response: RTS have replaced the term retrogressive thaw slump throughout the text, after the term has been defined on line 80.

Line 130: Same than for the Abstract, please add "Canada"

Response: Canada has been specified (now line 139).

Results
Lines 307-308: Can you indicated the DOY corresponding to the periods that you evoked ("end of July", "middle of July") to be consistent with the Figure 2.

Response: Three periods have been identified and DOY have been added as follows "*During the measurement period (Table 1) T_a increased from 10.5°C in the early season (DOY=175-185) to 12.2°C during the peak of the growing season (DOY=186-202) and then decreased to 7.2°C by the end of July (DOY=203-210).*" (Now lines 358-360).

Lines 321-322: This explanation for the choice of the three periods should appeared before (in 3.1).

Response: The description and explanation of the three distinct periods has been

moved to section 3.1 (lines 355-358).

Response: This sentence has been rewritten for clarity as follows "*Arctic sites show significant inter-annual variability, which is controlled by temperature; increased temperatures may result in enhanced emissions ...*" (lines 539-541).

References

Burba, G. G., McDermitt, D. K., Grelle, A., Anderson, D. J., & Xu, L. (2008). Addressing the influence of instrument surface heat exchange on the measurements of CO_2 flux from open-path gas analyzers. Global Change Biology, 14(8), 1854-1876.

Burba, G., D. McDermitt, J. Hupp, D. Anderson, & R. Eckles. (2010). Solution for Minimizing Surface Heating Effect for Fast Open-path CO_2 Flux Measurements in Cold Environments. American Geophysical Union Fall Meeting, San Francisco, California, 13-17 December.

Lantz, T. C., and S. V. Kokelj (2008). Increasing rates of retrogressive thaw slump activity in the Mackenzie Delta region, N.W.T., Canada, Geophys. Res. Lett., 35, L06502, doi:10.1029/2007GL032433.

Lewkowicz, A. G. (1990). Morphology, frequency and magnitude of active-layer detachment slides, Fosheim Peninsula, Ellesmere Island, N.W.T., Nordicana, 54, 111–118, 1990.

Lewkowicz, A. G. and Harris, C. (2005). Frequency and magnitude of active-layer detachment failures in discontinuous and continuous permafrost, northern Canada, Permafr. Periglac. Process., 16(1), 115–130..

Zha, T., Barr, A.G., Black, T.A., McCaughey, J.H., Bhatti, J.S., Hawthorne, I., Krishnan, P., Kidston, J., Saigusa, N., Shashkov, A., & Nesic, Z. (2009). Carbon sequestration in boreal jack pine stands following harvesting. Global Change Biology 15(6): 1475-1487.

1   Title: The effect of a permafrost disturbance on growing-season carbon-dioxide fluxes in

2   a high Arctic tundra ecosystem

3   Running Head: Permafrost disturbance and CO_2 fluxes

4   Authors: Cassidy, AE, Christen, A, Henry, GHR

5   Institute: Department of Geography, The University of British Columbia,

6   1984 West Mall, Vancouver, British Columbia, Canada, V6T1Z2

7   Corresponding Author: AE Cassidy

8   Telephone: +001 778 840 3018

9   Email: alison.cassidy@geog.ubc.ca

10   Keywords: eddy covariance, permafrost disturbance, thermokarst, net ecosystem

11   exchange, retrogressive thaw slump, tundra ecosystem

12   Manuscript Type: Research Article

13

14

15

16

17

18

19

20

21

22

23

24   **Abstract**

25   Soil carbon stored in high-latitude permafrost landscapes is threatened by warming, and

26   could contribute significant amounts of carbon to the atmosphere and hydrosphere as

27   permafrost thaws. Thermokarst and permafrost disturbances, especially active layer

28   detachments and retrogressive thaw slumps, are present across the Fosheim Peninsula,

29   Ellesmere Island, Canada. To determine the effects of retrogressive thaw slumps on net

30   ecosystem exchange (NEE) of CO_2 in high Arctic tundra, we used two eddy covariance

31   (EC) tower systems to simultaneously and continuously measure CO_2 fluxes from a

32   disturbed site and the surrounding undisturbed tundra. During the 32- day measurement

33   period in the 2014 growing season the undisturbed tundra was a small net sink (NEE = -

34   0.1 g C m^{-2} d^{-1}); however, the disturbed terrain of the retrogressive thaw slump was a net

35   source (NEE = +0.4 g C m^{-2} d^{-1}). Over the measurement period, the undisturbed tundra

36   sequestered 3.8 g C m^{-2}, while the disturbed tundra released 12.5 g C m^{-2}. Before full leaf

37   out in early July, the undisturbed tundra was a small source of CO_2, but shifted to a sink

38   for the remainder of the sampling season (July), whereas the disturbed tundra remained a

39   source of CO_2 throughout the season. A static chamber system was also used to measure

40   fluxes in the footprints of the two towers, in both disturbed and undisturbed tundra, and

41   fluxes were partitioned into ecosystem respiration (R_e) and gross primary production

42   (GPP). Average GPP and R_e found in disturbed tundra were smaller (+0.40 μmol m^{-2} s^{-1}

43   and +0.55 μmol m^{-2} s^{-1}, respectively) than those found in undisturbed tundra (+1.19 μmol

44   m^{-2} s^{-1} and +1.04 μmol m^{-2} s^{-1}, respectively). Our measurements indicated clearly that the

45   permafrost disturbance changed the high Arctic tundra system from a sink to a source for

46   CO_2 during the growing season.

1   Introduction

Permafrost soils in the Arctic store vast amounts of carbon. The northern permafrost zone carbon inventory estimates the quantity of soil organic carbon stored in the top 3 m of frozen and unfrozen soils in northern circumpolar permafrost regions to be 1035 ±150 Pg, or approximately 50% of worldwide soil organic carbon (Tarnocai et al., 2009, Grosse et al., 2011, Hugelius et al., 2013, Schuur et al., 2015). Measurement difficulties and uncertainty regarding carbon storage in cryoturbated soils may result in an underestimation of current estimates, by as much as a factor of two (Hugelius et al., 2013). As ground temperatures increase due to global climate change and permafrost thaws, this organic carbon becomes available for microbial decomposition (Schuur et al., 2008). McGuire et al. (2006) noted the implications for feedbacks to Arctic climate resulting from disturbance and enhanced decomposition including positive feedbacks as more CO_2 released leads to warmer temperatures, thus exacerbating thaw and leading to further release of CO_2. Conversely, a negative feedback may result if soil carbon inputs offset decomposition, as the balance between litter accumulation and decomposition determines the net effect on climate (Davidson et al., 2006, Cornelissen et al., 2007).

Predicted climate change is expected to increase the frequency and extent of land surface disturbances in the Arctic (ACIA, 2005, Vincent et al., 2011). These disturbances are usually linked to thermokarst and affect soil temperature, water quality and soil nutrients (Mackay, 1970, Lamoureux and Lafrenière, 2009, Lantz et al., 2009, Kokelj and Lewkowicz, 1998, Kokelj and Lewkowicz, 1999). In the High Arctic, these disturbances commonly take the form of retrogressive thaw slumps (RTS). RTS are initiated by the exposure of ground ice (sometimes linked to coastal erosion) and result in the removal of

71 soil and vegetation as the slump retreats further upslope (Lantuit and Pollard, 2008). As

72 ground ice thaws, the headwall regresses and will remain active until falling blocks of

73 soil and vegetation insulate exposed ice and prevent further thaw (Burn and Friele, 1989).

74 Within the overall landscape, these distinct landforms often create unique microclimates

75 resulting in increased landscape heterogeneity (Ukraintseva, 2008, Lantz et al., 2009,

76 Bosquet, 2011). Climate warming may cause differential responses in disturbed and

77 undisturbed tundra. For example, the response of plants to increases in temperature may

78 be intensified when disturbance occurs (Lantz et al., 2009). Lantz et al. (2009) suggested

79 disturbances play a more significant role in vegetation modification than temperature

80 changes, particularly at the fine scale. We hypothesize that those changes in the landscape

81 (slumping and vegetation loss) will have a significant effect on the carbon balance of

82 tundra systems. However, no direct measurements of net ecosystem exchange (NEE) and

83 its component fluxes, ecosystem respiration (R_e) and gross primary productivity (GPP),

84 have been completed to determine the effect of these permafrost disturbances.

85   Eddy covariance (EC) has been used to quantify NEE in the Arctic and

86 measurements vary greatly, depending on location and ecosystem type. The magnitude

87 of CO_2 fluxes are generally greater at low latitudes than in the high Arctic (Lafleur et al.,

88 2012) and in wet sedge areas than dry heath tundra (Kwon et al., 2006; Groendahl et al.,

89 2007). Variability may be explained by nutrient availability, substrate quantity and soil

90 organic matter (Mbufong et al., 2014). Typical mean daily values measured during the

91 growing season ranged between 0.2 and 2.2 g C m^{-2} d^{-1} at a wide range of Arctic sites

92 (Lafleur et al., 2012). Previous studies have found large inter-annual variability within

93 and among sites, which can shift the site from a carbon sink to carbon source (Griffis and

94 Rouse, 2001; Kwon et al., 2006; Merbold et al., 2009). Large variability in tundra

95 vegetation communities over short distances increases difficulty in assessing NEE fluxes

96 across the Arctic, and determining their responses to disturbance and environmental

97 change (Lafleur et al., 2012).

98   Static chamber systems, which partition NEE into component fluxes GPP and R_e,

99 are an alternative method of measuring ecosystem fluxes. Chamber studies in the Arctic

100 have found a loss of carbon during the winter, and increasing sink potential with a longer

101 growing season (Welker et al., 2000; Welker et al., 2004). At Alexandra Fiord, Ellesmere

102 Island, experimental warming impacted NEE differently based on soil moisture, with a

103 greater increase in respiration in dry than wet sites (Welker et al., 2004). Across a

104 latitudinal gradient, warming tended to increase respiration, with the greatest increases

105 found in dry ecosystems (Oberbauer et al., 2007).

106   While NEE values are generally similar between chamber and EC methods,

107 differences are attributed to the scale of the measurements (Stoy et al., 2013). Fox et al.

108 (2008) showed there was large bias in upscaling chamber measurements, relative to EC

109 values in a tundra ecosystem, due to microscale surface heterogeneity of the landscape.

110 Further, with 24 hours of daylight during which the sun remains relatively high above the

111 horizon, the usual partitioning methods for EC measurements into component fluxes

112 (Reichstein et al., 2012) are not applicable, as they rely on nighttime measurements, or

113 measurement during low light conditions. Consequently, to measure the impact of the

114 RTS on the CO_2 exchange of the high Arctic tundra we used both EC and chamber

115 measurements.

116   In this study, we analyze the impacts of RTS on CO_2 exchange in a high Arctic

117   tundra ecosystem. Our main research objective was to examine how growing season NEE

118   and its component fluxes vary between a RTS and undisturbed tundra.

119

120   **1.1   Study Area**

121

122   Our research was conducted on the Fosheim Peninsula, located on western Ellesmere

123   Island, Canada (79° 58' 56" N 84° 23' 55" W (WGS-84), elevation 100 m asl). The field

124   site had an isolated retrogressive thaw slump (RTS) (6300 m^2) within a relatively flat area

125   and wind patterns were constrained (NNE-SSW) by its location near a shallow valley

126   bottom (Fig. A1). Ice-rich permafrost is found throughout the study region and increased

127   summer temperatures and precipitation over the past 20 years have resulted in greater

128   occurrence of active layer detachment slides and RTS (Lewkowicz and Harris, 2005a).

129   The geological substrate is mainly sandstones of the Eureka Sound group (Bell, 1996)

130   with marine deposits of silts and fluvial sandy soils varying in thickness above bedrock

131   (Robinson and Pollard, 1998). The limit of ocean inundation at the end of the last

132   glaciation in the area lies at approximately 140 m above sea level (Bell, 1996), with

133   limited vegetation above this level; our study location was located below the marine

134   limit. Vegetation at the site was a relatively uniform dwarf-shrub-graminoid community

135   on moderately drained, slightly alkaline soils. Vegetation located in the undisturbed

136   tundra was dominated by *Salix arctica, Dryas integrifolia, Carex nardina*, moss, and

137   lichen. Within the disturbance, the dominant plant species was *Puccinellia angustata*,

138   which is able to colonize the disturbed area and proliferate. Vegetation cover within the

139   RTS varied based on moisture and proximity to undisturbed vegetation, and was much

140   lower than the surrounding undisturbed areas (with estimates of cover averaging (±SE)

141   3(±0.5)% and 27(±1.5)% total cover, respectively). The nearest weather station, Eureka,

142   is located 40 km to the west and has a mean temperature of 6.1°C and mean precipitation

143   of 14.5 mm in July over the 1981-2010 period (Environment Canada, 2015).

2   Materials and Methods

2.1   Eddy covariance measurements of carbon-dioxide fluxes

An appropriate sampling design was necessary to quantify the CO_2 fluxes between land surface and atmosphere simultaneously from disturbed and undisturbed sites in close proximity (Hollinger and Richardson, 2005). We used a dual eddy covariance approach, which was advantageous over a single eddy covariance tower as we were able to measure fluxes simultaneously from disturbed tundra and the surrounding undisturbed tundra (Fig. 1; Fig. 2). However, direct placement of an EC system within the disturbance was not possible due to the active mass movements in the RTS creating risk for researchers and equipment. Two towers were established on opposite sides of the RTS, at the boundary between disturbed and undisturbed terrain (Fig. 1). Tower 1 was established on the southern boundary of the RTS and Tower 2 was established on the northern boundary at a distance of 90 m from Tower 1. Disturbed tundra were areas impacted by RTS, while undisturbed tundra were areas located outside the boundary of the RTS. This set-up allowed the measurement of fluxes containing signals from both areas simultaneously. By using turbulent source area modeling (see below) we then estimated the contribution of disturbed and undisturbed tundra to each of the signals.

Both EC systems were established on tripods located on the periphery of the active RTS on 26 June 2014 and operated continuously until 28 July 2014. On each system the instrumentation included: an ultrasonic anemometer (CSAT-3, Campbell Scientific Inc., Logan, UT, USA) and a co-located infrared gas analyzer (IRGA) (LI-7500, LI-COR Inc., Lincoln, NE, USA). The IRGA was tilted 30° from the vertical to minimize issues associated with sensor heating and reduce pooling of moisture on the windows. Both IRGA and ultrasonic anemometer were established at a height of 1.3 m on both towers; a

8

168   temperature and humidity sensor (HMP, Campbell Scientific Inc.) at 1m; a quantum

169   sensor (SQ-110, Apogee Instruments Inc., Logan, UT, USA; height: 1m); a net

170   radiometer (NR Lite, Kipp & Zonen B.V., Delft, The Netherlands; height: 1m); and all

171   sensors were attached to a data logger (CR1000, Campbell Scientific Inc.). This double

172   EC sampling technique allowed for simultaneous sampling of fluxes from the disturbed

173   tundra and the surrounding undisturbed (control) terrain for most time steps. Previous

174   knowledge of wind direction ϑ based on the location of the disturbance within a valley

175   constrained winds along the valley axis into up-valley wind ($0º < \vartheta < 40º$) and down-

176   valley wind ($160º < \vartheta < 200º$) directions, which resulted in aligning the sector facing

177   towards 290°, having a sector free of flow distortion from 140º to 80º (distorted sector

178   80º to 140º). The towers were established at a distance of 3 m from the slump edge to

179   ensure stability, and were moved periodically throughout the season due to recession of

180   the slump edge. Additionally, the potential impacts of step changes due to the placement

181   of the flux tower at the boundary of disturbed and undisturbed tundra was minimized

182   through the use of friction velocity thresholds and removing data with wind along the

183   discontinuity with obvious flow distortion. Both IRGAs were calibrated prior to the field

184   season using a two-point calibration in the lab against standards from the Greenhouse Gas

185   Measurement Laboratory (GGML), Meteorological Service of Canada using a zero gas

186   and span gas of known mixing ratio.

187   Fluxes of CO_2 (F_C) were computed in EddyPro® (V5.1.1, LI-COR Inc.) with a

188   missing sample allowance of 30%. F_C was calculated over a 30 minute averaging interval

189   using double rotation for tilt correction, block average detrending, contact time lag

9

190 detection, and density corrections using mixing ratios (Burba et al., 2012). Data were

191 quality checked using the flagging system proposed by Mauder and Foken (2004).

192 **2.2 Turbulent source area model**

193
194 To estimate the instantaneous turbulent source area that influences sampled NEE, a 2-

195 dimensional gradient diffusion and crosswind dispersion model (Kormann & Meixner,

196 2001) was run for all 30 min periods between 26 June 2014 and 28 July 2014 at a 1 m

197 grid resolution over a domain of 300 x 300 m with the tower situated in the centre (see

198 Fig. 2). Model inputs included wind direction ϑ (º), standard deviation of the lateral wind

199 component σ_v (m), roughness length z_0 (m) and Obukhov length L (m) separately for

200 each tower and for each time step. ϑ, σ_v and L were calculated directly by EddyPro®

201 based on measurements by the two ultrasonic anemometers. Roughness length varied

202 depending on whether the upwind surface in a particular time period was in the RTS or

203 representing undisturbed tundra. z_0 was determined separately for 10º wind direction bins

204 based on the ensemble of measurements from the entire dataset following Paul-Limoges

205 *et al.* (2013). For each wind sector ϑ, z_0 was calculated for cases with near-neutral

206 stability (-0.05 < z/L < +0.05) using Eq. 1:

$$z_0(\vartheta) = z \ \exp\left(-\frac{k\bar{u}}{u_*}\right) \tag{1}$$

207
208   where z is the measurement height (1.3 m), k is the von Kármán constant (0.4), $\bar{u}$ is

209 the measured mean horizontal wind (m s⁻¹) from this wind direction, and u_* is the

210 simultaneously measured friction velocity (m s⁻¹) calculated as $u_* = (\overline{u'w'}^2 + \overline{v'w'}^2)^{0.25}$

211 where $\overline{u'w'}$ and $\overline{v'w'}$ are covariances of longitudinal (u), lateral (v) and vertical (w) wind

212   components. Mean wind $\bar{u}$ and covariances were calculated by EddyPro[®] based on

213   measurements from the ultrasonic anemometer. The disturbed sectors of both towers had

214   an average $z_0 = 0.032$ m whereas the undisturbed sectors had an average $z_0 = 0.017$ m.

215   Gridded flux footprints (or vertical per unit point source) ϕ *(x,y)* were calculated in with 1

216   m resolution for each 30 min step following Christen et al. (2011). A fraction of the flux

217   footprint was predicted to be outside the 300 m study area, which was assumed to

218   represent an undisturbed (control) surface (as no additional permafrost disturbances were

219   located within proximity of the towers).

220   The 300 m x 300 m model domain included the entire disturbance and a spatial mask

221   I (x,y) of the domain was created with a value of 1 inside the disturbance boundary and 0

222   for undisturbed tundra. For each grid-cell, I (x,y) was multiplied by ϕ (x,y), and then

223   summed to determine the fraction of the footprint that originates from inside the RTS

224   (Eq. 2):

$$\Phi_d = \sum_{x=1}^{300} \sum_{y=1}^{300} I(x,y)\phi(x,y) \tag{2}$$

225

226   Φ_d is the fraction of the tower signal (from 0 to 1) influenced by the disturbed surface

227   of the RTS. The fraction of the signal influenced by the undisturbed tundra Φ_c is then

228   calculated as $\Phi_c = 1 - \Phi_d$. By solving a set of linear equations (Eq. 3 and Eq. 4), we

229   are able to partition the component fluxes of CO_2 (Fig. 2) from the disturbed tundra

230   (NEE$_d$) and from the undisturbed tundra (NEE$_c$) from both towers (T1 and T2):

$$NEE(T1) = \Phi_d(T1)NEE_d + \Phi_c(T1)NEE_c \tag{3}$$

231

$$\text{NEE(T2)} = \Phi_d(\text{T2})\text{NEE}_d + \Phi_c(\text{T2})\text{NEE}_c \tag{4}$$

232　　Turbulent source areas calculated for each time step over the sampling period are

233　shown in Fig. 2. These two example time steps from Fig. 2 can be solved as follows. In

234　the first time-step (09:00), Φ_c for T1 is 1, therefore the NEE(T1) = NEE_c = -0.17 μmol

235　m^{-2} s^{-1}. For T2, 88% (Φ_d) was disturbed while the remaining 12% was allocated as

236　undisturbed (Φ_c), so NEE$_c$ and NEE$_d$ were solved with NEE(T2) = 1.20 μmol m^{-2}s^{-1} and

237　resulted in NEE$_d$ = 1.39 μmol m^{-2} s^{-1}. Corresponding to the second time step from Fig.

238　A1 (18:00), T1 is influenced by both undisturbed and disturbed NEE as Φ_d $(T1)$ = 0.73

239　and Φ_c $(T1)$ = 0.27 and NEE(T1) is 0.38 μmol m^{-2} s^{-1}. At T2, Φ_d is 0, while Φ_c is 1, so

240　NEE(T2) = NEE$_c$ = -0.03 μmol m^{-2} s^{-1}. Consequently, NEE$_c$ = -0.03 μmol m^{-2}s^{-1} and

241　NEE$_d$ = 0.54 μmol m^{-2}s^{-1}.

242　　Calculations of NEE$_d$ and NEE$_c$ were numerically unstable under multiple

243　combinations of surface fractions, including when winds were parallel to the edge of the

244　disturbance and when Φ_d and Φ_c were roughly equal to one another. As a result, values

245　where the absolute difference between Φ_d and Φ_c was less than 0.05 were removed and

246　fluxes were gap-filled as detailed below during these periods.

247　　The resulting NEE$_c$ and NEE$_d$ were compared and fluxes that had a difference from

248　the daily average that was greater than 5 standard deviations of the 30 min values of the

249　same day (applied iteratively) were removed. For further analysis, half hour fluxes were

250　averaged to calculate hourly fluxes. If one of the two 30 min values was invalidated, then

251　the hourly value was calculated based on the remaining other 30 min period. Hourly gaps

252　that still existed were then filled using the following methods: a) gaps in NEE$_c$ and NEE$_d$

253　of less than 2 hours were filled using a linear interpolation; and b) gaps greater than 2

12

254   hours were filled using aggregate averaging over a rolling three-day window selecting the

255   same time of the day. The cleaned and filled dataset is composed of 86% original data

256   and 14% gap filled (of a total of 750 data points, 106 of these were modeled). Data were

257   also removed during times of maintenance, when the towers were moved and when

258   manual chamber or vegetation measurements were made within the tower footprint.

259   **2.3   Portable chamber system**

260
261   On 27 June 2014, 63 opaque PVC collars (10 cm diameter, $A = 78.5$ cm^2, 6 cm depth)

262   were installed across the source areas of T1 and T2, in both the disturbed and undisturbed

263   zones (disturbed tundra N=21, undisturbed tundra N=42). They were inserted 4 cm into

264   the ground so as to minimally disturb soil and vegetation and left to protrude 2 cm above

265   the soil surface. As moss cover was minimal and discontinuous, the location of the

266   ground surface could be easily identified as the upper surface of the soil. Collar locations

267   were randomly determined based on the generation of random distances and angles from

268   the flux tower within disturbed and undisturbed flux source areas, with a minimum

269   distance of 2 m and a maximum distance of 30 m from the towers. The disturbed areas of

270   the RTS were not entirely devoid of vegetation, as clumps of soil and plants existed

271   sporadically throughout the disturbance; 9 of 21 collars contained at least one individual

272   plant. Measurements of CO_2 fluxes began on 29 June, to allow the immediate disturbance

273   effects of installation to dissipate.

274   A non-steady state vented portable chamber system similar to Jassal *et al.*(2005)

275   was used to measure fluxes from each collar using transparent and opaque chambers. The

276   measurement head was a PVC chamber with a volume of 1.4 x 10^{-3} m^3 (height: 15.6 cm,

277   diameter: 10.7 cm). Fluxes from all collars were measured six times throughout the study

278   period, at 5-day intervals. The chamber head was placed on each collar and a foam

279   gasket sealed the connection between the collar and the chamber head. Measurements

280   were made for two minutes. A pump (flow rate 600 cm^3 min^{-1}) circulated air from the

281   chamber head into a portable, battery operated infrared gas analyzer (IRGA) (LI-840, LI-

282   COR Inc., Lincoln, USA) and back into the chamber head through a closed circuit. The

283   IRGA determined CO_2 mixing ratios ([CO_2] in ppm) and water vapour concentrations at a

284   temporal resolution of 1 Hz during the run. The IRGA was calibrated in the laboratory

285   prior to sampling using a two-point calibration, against standards from the Greenhouse

286   Gas Measurement Laboratory (GGML), Meteorological Service of Canada, using a zero

287   gas and span gas of known mixing ratio. The IRGA has been calibrated in the laboratory

288   for effective volume, which exceeds geometric volume by 10% due to absorption of CO2

289   on the walls of the chamber and contribution of near-surface soil porosity (Jassal et al.,

290   2012). This calibration was carried out in the laboratory by determining the difference

291   between two flux measurements, one immediately following the other, where the second

292   measurement included a known rate of injection of CO_2 into the chamber.

293   Fluxes were calculated from $\Delta[CO_2]/\Delta t$ (linear regression over 2 min, discarding

294   the first 10 seconds), using Eq. 5:

$$Fc = \frac{\rho \, \overline{D} V}{A} \frac{\Delta[CO_2]}{\Delta t} \qquad (5)$$

295

296   where ρ is molar air density (mol m^{-3}) calculated from measured air temperature, D is

297   dilution considering [H_2O], $\Delta[CO_2]/\Delta t$ is the rate of change in CO_2 mixing ratio over

298   time (μmol mol^{-1} s^{-1}), and V and A are chamber volume and area, respectively. To obtain

299   measurements of NEE, the transparent chamber head was used on each collar. For

300   ecosystem respiration (R_e) measurements, the chamber was removed and allowed to

301   equilibrate to ambient [CO_2] before being replaced on the collar, and a shroud was placed

302   over the transparent chamber head to block out all PAR. GPP was calculated based on

303    $GPP = R_e - NEE$, where NEE is negative if $GPP > R_e$ and both R_e and GPP are positive

304   values. NEE and R_e measurements were taken within minutes at each collar allowing for

305   comparison. Measurements were completed over a 7-hour sampling period and were

306   always completed between 10:00 and 18:00 CDT to reduce diurnal changes in light and

307   temperature.

308   **2.4   Environmental Variable Sampling**

309
310   Soil temperature loggers (HOBO Pendant Temperature/Light Data Loggers, Onset

311   Computer Corporation, Bourne, MA, USA) were installed at randomly selected collars

312   throughout the study area within 0.5 m of the collar. A total of 21 HOBO sensors (14

313   sensors located in undisturbed tundra and 7 sensors in disturbed tundra) measured soil

314   temperatures at 5 cm every minute throughout the sampling season. The soil temperatures

315   were aggregated into hourly averages to allow for comparison with hourly EC data. Soil

316   moisture was measured adjacent to collars every five days as volumetric water content

317   (%) using a Time Domain Reflectometry (TDR) sensor (HydroSenseII Soil Water TDR,

318   Campbell Scientific Inc., Logan, UT, USA) with 12 cm rods. After rain events,

319   measurements were delayed for 24 hours.

320

3 Results

3.1 Environmental conditions during the study period

The measured variations over the study period in air temperature (T_a), net radiation (Q^*, over undisturbed tundra), incoming photosynthetically active radiation (PAR), and vapour pressure deficit (VPD) measured at Tower 2, and soil temperature from the disturbance and undisturbed tundra area near Tower 2 are shown in Fig. 3. The early season was characterized by clear skies, however the middle of July was dominated by a period of cloudy, cooler conditions (exemplified by decreased Q^*, Fig. 3). Air and soil temperatures showed distinct diurnal and seasonal patterns (Fig. 3; Fig. 4), characterized by an increase in both temperatures early in the season, which were sustained through the peak season, followed by decreases in both during the end of the season. Three distinct periods (early, peak and late season) were identified throughout the study period based on plant phenological development and environmental conditions (Fig. 3; Fig. 4). These periods varied in their duration (see Table 1). During the measurement period, T_a increased from 10.5ºC in the early season (DOY=175-185) to 12.2°C during the peak of the growing season (DOY=186-202) and then decreased to 7.2°C by the end of July. On a diurnal basis, disturbed soils reached greater temperatures than undisturbed soils earlier in the season (12.6°C and 11.6°C, respectively), but cooled off quickly later in the season (7.8°C and 8.1°C, respectively), due to the lack of insulating vegetation (Mann Whitney U-Test ($V = 181992$, $p < 0.01$)). In undisturbed terrain, soil moisture decreased during peak season, while soil moisture increased steadily in disturbed tundra (Table 1). Overall, soil moisture values were significantly greater (Mann Whitney U-Test ($V = 7023$, $p < 0.01$)) in disturbed soils (24.1% ± 0.9) than in undisturbed soils (13.9% ± 0.4).

3.2 NEE of disturbed and undisturbed tundra

The early season was characterized by leaf emergence, cool temperatures, and elevated soil moisture (Table 1) due to recent snowmelt. The peak season was characterized by maximum leaf area and flowering of vegetation (e.g. *Salix arctica*, *Dryas integrifolia,* and grass species) and a decrease in surface soil moisture as warm air temperatures and large VPD persisted. The late season was characterized by the beginning of leaf senescence, dry soils, and the greatest active layer depth. Precipitation was minimal throughout the season (1.2 mm at Eureka), with isolated rain events occurring on July 17, 21, and 26. There was a significant windstorm beginning on 22 July and that lasted 24 hours, with wind speeds (as determined from the raw 20 Hz spikes) of up to 21 m s^{-1}.

NEE_c and NEE_d were analyzed separately for three periods (early, peak and late season). In the undisturbed tundra, NEE_c was initially a small source in the early period and transitioned to a small sink as photosynthesis increased during the peak season. In the late season, NEE_c became a small source consistent with decreased air and soil temperatures and the beginning of leaf senescence. This was in contrast with fluxes measured in the disturbed area (NEE_d), which remained a CO_2 source throughout the sampling period and displayed only slightly dampened values during peak season. Overall, NEE_c and NEE_d were significantly different throughout the sampling period (Mann-Whitney U-Test ($V = 45839$, $p < 0.01$)).

Aggregate fluxes calculated over the study period showed an overall loss of CO_2 from disturbed tundra, and a modest CO_2 sink in the undisturbed tundra (Fig. 6). Daily averages of NEE_c ranged from -0.89 to +0.54 g C m^{-2} day^{-1}. NEE_d ranged from -0.29 to

369   +1.63 g C m^{-2} day^{-1}. During the early season, the average daily NEE$_c$ was a small source

370   of CO_2 to the atmosphere (+0.07 g C m^{-2} day^{-1}) while disturbed tundra was a greater

371   source of CO_2 (NEE$_d$ = +0.55 g C m^{-2} day^{-1}). During peak growth, this shifted as the

372   undisturbed tundra sequestered -0.29 g C m^{-2} day^{-1} and disturbed tundra continued to emit

373   CO_2 at an average of +0.26 g C m^{-2} day^{-1}. During the end of the sampling season, the

374   undisturbed was a very small sink of CO_2 with mean NEE of -0.02 g C m^{-2} day^{-1} and the

375   NEE of the disturbed tundra was +0.47 g C m^{-2} day^{-1}. Over the duration of the entire

376   sampling period, the disturbed tundra was a source of CO_2 with an average of +0.39 g C

377   m^{-2} day^{-1} while the undisturbed tundra was a sink for CO_2 with an average uptake of -0.12

378   g C m^{-2} day^{-1} (Fig. 5). In total, the undisturbed tundra sequestered 3.8 g C m^{-2}, while the

379   disturbed tundra released 12.5 g C m^{-2} over the 32-day measurement period.

380   Diurnal NEE from the tower systems correspond with soil temperatures. In

381   disturbed areas, as soil temperatures warmed, CO_2 emissions increased, consistent with

382   increased respiration. However, fluxes in undisturbed areas showed increased

383   sequestration during midday, due to greater photosynthetic activity dominating over

384   respiration increases.

385   Temporal patterns of fluxes and climatic and environmental variables were

386   analyzed for disturbed and undisturbed areas. In the disturbed area, regression analysis

387   revealed strong relationships between NEE and soil temperature, PAR, T_a and VPD for

388   the early and peak season periods (p<0.001), while PAR was the most important control

389   during the late season (r^2=0.50, p < 0.001). Over the undisturbed tundra, correlations

390   between NEE and environmental variables varied throughout the sampling period. During

391   the early season, PAR was most strongly correlated (r^2=0.16, p<0.001) with NEE,

392 however, during the peak season temperature (r^2=0.08, p<0.001) and vapour pressure

393 deficit (VPD) (r^2=0.08, p<0.001) became important controls on NEE. At the end of the

394 sampling season once again PAR was most strongly correlated with NEE (r^2=0.25,

395 p<0.001) in the undisturbed tundra.

396 **3.3   Partitioning of NEE**

397

398   Measurements from the static chamber system were allocated to one of the three

399 seasonal periods, allowing comparison with EC data (Fig. 7). The NEE values measured

400 using the chamber technique supported the EC measurements, but allowed fluxes to be

401 partitioned into their component parts. The chamber measurements showed that the

402 magnitude of GPP and R_e were roughly similar, resulting in minimal NEE in both

403 disturbed and undisturbed areas (Table 2; Fig. 8). Variability in GPP was greater in the

404 undisturbed tundra with values up to 8.03 μmol m^{-2} s^{-1} while the maximum GPP in the

405 disturbed tundra reached 2.47 μmol m^{-2} s^{-1}. R_e ranged up to +5.92 μmol m^{-2} s^{-1} in the

406 undisturbed tundra and to +2.23 μmol m^{-2} s^{-1} in the disturbed tundra. Over the sampling

407 season in the disturbed areas, chamber-measured GPP averaged 0.40 μmol m^{-2} s^{-1}

408 increasing during peak season to 0.45 μmol m^{-2} s^{-1}, before falling to 0.24 μmol m^{-2} s^{-1} in

409 the late season. Respiration was greatest during the early season with +0.70 μmol m^{-2} s^{-1},

410 decreasing to +0.53 μmol m^{-2} s^{-1} during peak season, and finally to +0.35 μmol m^{-2} s^{-1}

411 during the late season. These opposing fluxes resulted in the disturbed tundra being a

412 small source for CO_2 throughout the entire sampling season. NEE measured by the

413 chamber system varied between +0.05 and +0.41 μmol m^{-2} s^{-1} in the disturbance with the

414 largest NEE occurring early in the season due to high respiration. R_e was always greater

415 in magnitude than GPP over disturbed tundra resulting in positive NEE values.

416   The undisturbed areas were small sources of CO_2 early in the season as R_e

417   outpaced productivity. In the undisturbed tundra, during the early season GPP averaged

418   0.85 μmol m^{-2} s^{-1}, nearly doubling during peak season to 1.47 μmol m^{-2} s^{-1}, before falling

419   to 1.00 μmol m^{-2} s^{-1} late in the season. R_e in the undisturbed tundra ranged from +0.62

420   μmol m^{-2} s^{-1} to +1.14 μmol m^{-2} s^{-1}, with the greatest respiration occurring during peak

421   growth. Both GPP and R_e peaked during the middle of the sampling period (mid July),

422   before decreasing at the end of the season, but GPP was always greater in magnitude than

423   R_e.

424

4 Discussion

During the 2014 growing season, the RTS at our high Arctic site was a CO_2 source while undisturbed tundra was a small sink. All fluxes were quite low, but similar to those measured in other high Arctic sites (Lafleur et al. 2012). Multi-year measurements of NEE in high Arctic tundra indicate that initial uptake of carbon coincides with snowmelt and increases in CO_2 emission rates correspond with deep and long-lasting snowpack (Lund et al., 2012). Arctic sites show significant inter-annual variability, which is controlled by temperature; increased temperatures may result in enhanced emissions (Griffis and Rouse, 2001; Kwon et al., 2006; Merbold et al., 2009; Lund et al., 2012). In the High Arctic, soil moisture differences result in variations in ecosystem respiration (measured using chamber systems) and may enhance the impacts of warming (Welker et al., 2004). Warming has been found to increase respiration along a latitudinal gradient with the greatest increases found in dry ecosystems (Oberbauer et al., 2007).

Based on chamber measurements, we found permafrost disturbance alters carbon dynamics by decreasing GPP and R_e (Fig. 7). However, reductions to GPP are greater than reductions to R_e, resulting in the disturbance becoming a net carbon source. Decreases in GPP are due to lower vegetation cover within disturbed terrain. Decreases in respiration have been found within slumps and slides and are linked with carbon export from the disturbed area (Abbott and Jones, 2015; Beamish et al., 2014). Respiration measured in other high Arctic polar desert sites was positively correlated with soil moisture (Emmerton et al., 2015). This balance between reduced R_e as a result of disturbance and potential increases as a result of increased soil moisture may result in the

448   greater magnitude of R_e relative to GPP and thus the overall shift to carbon source within

449   the disturbance.

450   Despite the small magnitude of these high Arctic fluxes, there was a considerable

451   effect of the permafrost disturbance as the net CO_2 emissions from the disturbance was

452   approximately three times larger than the net sequestration in the undisturbed tundra.

453   Overall, the double EC system approach coupled with a source area model proved to be

454   an effective method of accurately partitioning measured fluxes into undisturbed and

455   disturbed contributions, and values were consistent with the static chamber

456   measurements.

457   By separating the growing season into three periods related to plant phenology,

458   we were able to identify differences in NEE between undisturbed and disturbed tundra

459   throughout the growing season. Initial sampling corresponded with leaf emergence, and

460   as the season progressed, plant growth and leaf area increased, resulting in increased

461   photosynthetic activity. The changes in NEE also corresponded to differences in PAR

462   during the three periods of the growing season. These phenological changes, especially in

463   leaf emergence, growth and senescence, can be compared to the shift in CO_2 fluxes as

464   initially the undisturbed tundra was a source of CO_2, but during peak growth there was a

465   distinct shift to CO_2 sink. By the end of the sampling season, vegetation has begun to

466   senescence, and this was reflected in reduced sink strength of NEE_c in the undisturbed

467   tundra. The disturbed areas contained low vegetation cover, resulting in a very low

468   magnitude of GPP. Throughout the season, the environmental controls on CO_2 fluxes in

469   the disturbed tundra were PAR, T_a and VPD during the early and peak season, while PAR

470   was a control in the late season.

471   Estimates of landscape level impacts of permafrost disturbances in an 81 km^2 ice-

472   free land area on the Fosheim Peninsula, which included the area used for our study, were

473   determined from satellite imagery and ground truthing in 2013. The analyses revealed

474   that permafrost disturbances currently accounted for 0.34 km^2 or only 0.4% of the

475   landscape (A.C.A. Rudy, personal communication, 2015). Although the landscape area

476   directly impacted by disturbance at this time is minimal, indirect impacts such as the

477   lateral export of dissolved and particulate organic matter (hence, carbon) through streams

478   and the hydrologic network are also important (Lamoureux and Lafrenière, 2009, Kokelj

479   and Lewkowicz, 1998, Kokelj and Lewkowicz, 1999). The frequency and magnitude of

480   these land surface disturbances appear to be increasing across the Fosheim Peninsula (and

481   elsewhere in the Arctic) as a result of the warming climate, thus exacerbating these

482   impacts (Lewkowicz, 1990; Lewkowicz and Harris, 2005b; Lantz and Kokelj, 2008). The

483   increasing frequency and magnitude of these disturbances will affect the carbon balance

484   at the landscape scale and could result in increased net CO_2 emissions from these areas in

485   the future. Organic carbon stored within permafrost has the potential to be released to the

486   atmosphere as permafrost thaws (Schuur et al., 2008; Hicks Pries et al., 2011; Hicks Pries

487   et al., 2013). We quantified this release to the atmosphere and demonstrated that these

488   permafrost disturbances are sources of CO_2 over the measurement period during the

489   growing season.

490   Potentially, some of the carbon in the soils could also be released in form of

491   methane (Anisimov, 2007; IPCC, 2007; Walter Anthony et al., 2012). Soil oxygen

492   availability has been found to influence permafrost carbon that is released as both carbon-

493   dioxide and methane, and under aerobic conditions significantly more carbon is released

494 as CO_2 than CH_4 (Lee et al., 2012). We expect that methane release was relatively

495 minimal from both the undisturbed and disturbed sites because of the aerobic conditions

496 present in the moderately drained soils found in our study location. However, we also

497 expect increased release of carbon with the deepening of the active layer and the increase

498 in frequency and magnitude of permafrost disturbances. In addition, inorganic carbon

499 released with the dissolution of carbonates and weathering may result in ventilation of

500 CO_2 and thus increased emissions (Lovett et al., 2006; Perez-Priego et al., 2013; Serrano-

501 Ortiz et al., 2010). With increasing soil moisture, soil ventilation associated with

502 carbonates may increase overall R_e (Emmerton et al., 2015). However, slow carbon

503 evolution in tundra soils (as a result of the release of inorganic carbon from carbonates)

504 would limit this influence (Billings et al., 1977).

505   Due to logistical constraints, our sampling season was limited to approximately

506 30 days after snowmelt had occurred. As these disturbances were dynamic in nature, the

507 site could not be left alone as personnel were needed monitor the slide edge location and

508 adjust the equipment as needed. Leaving the site unmanned would have put the

509 equipment at risk. Shoulder season and winter respiration have been shown to be

510 significant in various studies for year-round estimates of the effects on the carbon cycle

511 (Nordstroem et al., 2001; Welker et al., 2004; Johansson et al., 2006; Humphreys and

512 Lafleur, 2011; Wang et al., 2011; Lund et al., 2012), however only growing season fluxes

513 were considered in our study. Starr and Oberbauer (2003) have found photosynthetic

514 activity in vascular plants under snow further indicating the importance of fluxes outside

515 the snow free period. These fluxes were not considered in our study and could alter the

516 annual carbon balance. However, year round measurements of carbon exchange in areas

517 impacted by permafrost thaw in Alaska indicate these areas act as sources of carbon over

518 multiple years (Vogel et al., 2009).

519 **5   Conclusion**

520

521   Using a dual EC sampling approach, in combination with the turbulent source

522 area model and complemented by static chamber measurements, we were able to

523 determine fluxes from one representative retrogressive thaw slump nearly continuously

524 over a majority of the 2014 growing season. We found that these disturbances modify the

525 NEE of the tundra, changing it from a net sink to a source of CO_2. The disturbance

526 reduced the magnitude of both R_e and GPP, although reductions to GPP were greater. The

527 dual EC approach in combination with the source area model allowed accurate

528 assessments of the contributions of disturbed and undisturbed areas to CO_2 fluxes so we

529 could quantify the effect of permafrost disturbance on NEE. This approach may be

530 preferable to measurements taken using manual portable chamber systems due to the

531 continuous sampling frequency and spatial integration of the signal.

532

533

534

535

536

537

538

539

540

Acknowledgements

References

564 **References**

565 Abbott, B. W. and Jones, J. B.: Permafrost collapse alters soil carbon stocks, respiration,
566 CH_4, and N_2O in upland tundra. Glob Chang. Biol, 21: 4570–4587.
567 doi:10.1111/gcb.13069, 2015.
568
569 ACIA: Arctic Climate Impact Assessment and Arctic Monitoring and Assessment
570 Programme and Program for the Conservation of Arctic Flora and Fauna and
571 International Arctic Science Committee, Cambridge University Press, New York, USA,
572 2005.
573
574 Anisimov, O. A.: Potential feedback of thawing permafrost to the global climate system
575 through methane emission, Environ. Res. Lett., 2, 045016, doi:10.1088/1748-
576 9326/2/4/045016, 2007.
577
578 Beamish, A., Neil, A., Wagner, I., Scott, N.A.: Short-term impacts of active layer
579 detachments on carbon exchange in a High Arctic ecosystem, Cape Bounty, Nunavut,
580 Canada, Pol. Biol., 37, 1459–1468, 2014.
581
582 Bell, T.: The last glaciation and sea level history of Fosheim Peninsula, Ellesmere Island,
583 Canadian High Arctic, Can. J. Earth Sci., 33, 1075-1086, 1996.
584
585 Billings, W. D. and Mooney, H. A.: The ecology of arctic and alpine plants, Biol. Rev.,
586 43, 481–529, doi:10.1111/j.1469-185X.1968.tb00968.x, 1968.
587
588 Billings, W.D., Peterson, K.M., Shaver, G.R. and Trent, A.W.: Root growth, respiration,
589 and carbon dioxide evolution in an arctic tundra soil, Arctic & Alp. Res., 9:129-137,
590 1977.
591
592 Bosquet, L.: The effects of observed and experimental climate change and permafrost
593 disturbance on tundra vegetation in the western Canadian High Arctic, Canadian theses,
594 Kingston, Ontario., 2011.
595
596 Burba, G., Schmidt, A., Scott, R. L., Nakai, T., Kathilankal, J., Fratini, G., Hanson, C.,
597 Law, B., McDermitt, D. K., Eckles, R., Furtaw, M. and Velgersdyk, M.: Calculating CO2
598 and H2O eddy covariance fluxes from an enclosed gas analyzer using an instantaneous
599 mixing ratio, Glob. Chang. Biol., 18, 385–399, doi:10.1111/j.1365-2486.2011.02536.x,
600 2012.
601
602 Burn, C. and Friele, P.: Geomorphology, Vegetation Succession, Soil Characteristics and
603 Permafrost in Retrogressive Thaw Slumps near Mayo, Yukon Territory, Arctic, 42(1),
604 31–40, 1989.
605
606 Christen, A., Coops, N. C., Crawford, B. R., Kellett, R., Liss, K. N., Olchovski, I., Tooke,
607 T. R., Van Der Laan, M. and Voogt, J. A.: Validation of modeled carbon-dioxide

emissions from an urban neighborhood with direct eddy-covariance measurements, Atmos. Environ., 45, 6057–6069, doi:10.1016/j.atmosenv.2011.07.040, 2011.

Cornelissen, J. H. C., Van Bodegom, P. M., Aerts, R., Callaghan, T. V., Van Logtestijn, R. S. P., Alatalo, J., Stuart Chapin, F., Gerdol, R., Gudmundsson, J., Gwynn-Jones, D., Hartley, A. E., Hik, D. S., Hofgaard, A., Jónsdóttir, I. S., Karlsson, S., Klein, J. A., Laundre, J., Magnusson, B., Michelsen, A., Molau, U., Onipchenko, V. G., Quested, H. M., Sandvik, S. M., Schmidt, I. K., Shaver, G. R., Solheim, B., Soudzilovskaia, N. A., Stenström, A., Tolvanen, A., Totland, Ø., Wada, N., Welker, J. M., Zhao, X., Brancaleoni, L., Brancaleoni, L., De Beus, M. A. H., Cooper, E. J., Dalen, L., Harte, J., Hobbie, S. E., Hoefsloot, G., Jägerbrand, A., Jonasson, S., Lee, J. A., Lindblad, K., Melillo, J. M., Neill, C., Press, M. C., Rozema, J. and Zielke, M.: Global negative vegetation feedback to climate warming responses of leaf litter decomposition rates in cold biomes, Ecol. Lett., 10, 619–627, doi:10.1111/j.1461-0248.2007.01051.x, 2007.

Davidson, E. A. and Janssens, I. A.: Temperature sensitivity of soil carbon decomposition and feedbacks to climate change., Nature, 440, 165–173, doi:10.1038/nature04514, 2006.

Edlund, S., Alt, B. and Young, K.: Interaction of climate, vegetation, and soil hydrology at Hot Weather Creek, Fosheim Peninsula, Ellesmere Island, Northwest Territories, Geol. Surv. Canada Curr. Res. 1989-D, 125-133, 1989.

Emmerton, C. A., St. Louis, V. L., Humphreys, E. R., Gamon, J. A., Barker, J. D. and Pastorello, G. Z.: Net ecosystem exchange of CO_2 with rapidly changing high Arctic landscapes. Glob Chang. Biol. Accepted Author Manuscript. doi:10.1111/gcb.13064, 2015.

Environment Canada, Canadian Climate Normals 1981-2010 Station Data, Environment Canada, available at: http://www.climate.weather.gc.ca (last access: 15 April 2015), 2015.

Fox, A. M., Huntley, B., Lloyd, C. R., Williams, M. and Baxter, R.: Net ecosystem exchange over heterogeneous Arctic tundra: Scaling between chamber and eddy covariance measurements, Global Biogeochem. Cy., 22, GB2027, doi:10.1029/2007GB003027, 2008.

Griffis, T. J. and Rouse, W. R.: Modelling the interannual variability of net ecosystem CO2 exchange at a subarctic sedge fen, Glob. Chang. Biol., 7(5), 511–530, 2001.

Groendahl, L., Friborg, T. and Soegaard, H.: Temperature and snow-melt controls on interannual variability in carbon exchange in the high Arctic, Theor. Appl. Climatol., 88, 111–125, doi:10.1007/s00704-005-0228-y, 2007.

Grosse, G., Harden, J., Turetsky, M., McGuire, A. D., Camill, P., Tarnocai, C., Frolking, S., Schuur, E. A. G., Jorgenson, T., Marchenko, S., Romanovsky, V., Wickland, K., French, N., Waldrop, M., Bourgeau-Chavez, L., and Striegl, R.G.: Vulnerability of high-

654 latitude soil organic carbon in North America to disturbance, J. Geophys. Res., 116,
655 G00K06, 2011.
656
657 Hicks Pries, C. E., Schuur, E. A. G. and Crummer, K. G.: Holocene Carbon Stocks and
658 Carbon Accumulation Rates Altered in Soils Undergoing Permafrost Thaw, Ecosystems,
659 15(1), 162–173, doi:10.1007/s10021-011-9500-4, 2011.
660
661 Hicks Pries, C. E., Schuur, E. a G. and Crummer, K. G.: Thawing permafrost increases
662 old soil and autotrophic respiration in tundra: partitioning ecosystem respiration using
663 δ(13) C and Δ(14) C., Glob. Chang. Biol., 19(2), 649–61, doi:10.1111/gcb.12058, 2013.
664
665 Hollinger, D. Y. and Richardson, A. D.: Uncertainty in eddy covariance measurements
666 and its application to physiological models., Tree Physiol., 25, 873–885,
667 doi:10.1093/treephys/25.7.873, 2005.
668
669 Hugelius, G., Tarnocai, C., Broll, G., Canadell, J. G., Kuhry, P. and Swanson, D. K.: The
670 northern circumpolar soil carbon database: Spatially distributed datasets of soil coverage
671 and soil carbon storage in the northern permafrost regions, Earth Syst. Sci. Data, 5, 3–13,
672 doi:10.5194/essd-5-3-2013, 2013.
673
674 Humphreys, E. and Lafleur, P.: Does earlier snowmelt lead to greater CO2 sequestration
675 in two low Arctic tundra ecosystems?, Geophys. Res. Lett., 38, L09703,
676 doi:10.1029/2011GL047339, 2011.
677
678 Jassal, R., Black, A., Novak, M., Morgenstern, K., Nesic, Z. and Gaumont-Guay, D.:
679 Relationship between soil CO2 concentrations and forest-floor CO2 effluxes, Agric. For.
680 Meteorol., 130, 176–192, doi:10.1016/j.agrformet.2005.03.005, 2005.
681
682 Jassal, R. S., Black, T. A., Nesic, Z., & Gaumont-Guay, D.: Using automated non-steady-
683 state chamber systems for making continuous long-term measurements of soil CO 2
684 efflux in forest ecosystems. Agric. For. Meteorol., 161, 57-65,
685 doi:10.1016/j.agrformet.2012.03.009, 2012.
686
687 Johansson, T., Malmer, N., Crill, P. M., Friborg, T., Åkerman, J. H., Mastepanov, M. and
688 Christensen, T. R.: Decadal vegetation changes in a northern peatland, greenhouse gas
689 fluxes and net radiative forcing, Glob. Chang. Biol., 12, 2352–2369, doi:10.1111/j.1365-
690 2486.2006.01267.x, 2006.
691
692 Kokelj, S. and Lewkowicz, A.: Long-term influence of active-layer detachment sliding on
693 permafrost slope hydrology, Hot Weather Creek, Ellesmere Island, Canada, … Int. Conf.
694 Permafrost, …, (55), 583–589, 1998.
695
696 Kokelj, S. and Lewkowicz, A.: Salinization of permafrost terrain due to natural
697 geomorphic disturbance, Fosheim Peninsula, Ellesmere Island, Arctic, 52(4), 372 – 385,
698 1999.
699

Kormann, R. and Meixner, F. X.: An analytical footprint model for non-neutral stratification, Boundary-Layer Meteorol., 99, 207–224, doi:10.1023/A:1018991015119, 2001.

Kwon, H.-J., Oechel, W. C., Zulueta, R. C. and Hastings, S. J.: Effects of climate variability on carbon sequestration among adjacent wet sedge tundra and moist tussock tundra ecosystems, J. Geophys. Res.- Biogeosciences, 111, G03014, doi: 10.1029/2005JG000036, 2006.

Lafleur, P., Humphreys, E., St Louis, V., Myklebust, M., Papakyriakou, T., Poissant, L., Barker, J., Pilote, M. and Swystun, K.: Variation in peak growing season net ecosystem production across the Canadian Arctic, Enviro Sci Tech, 46, 7971–7977, 2012.

Lamoureux, S. and Lafrenière, M.: Fluvial impact of extensive active layer detachments, Cape Bounty, Melville Island, Canada, Arctic, Antarct. Alp. Res., 41(1), 59–68, doi:10.1657/1523-0430-41.1.59, 2009.

Lantuit, H. and Pollard, W. H.: Fifty years of coastal erosion and retrogressive thaw slump activity on Herschel Island, southern Beaufort Sea, Yukon Territory, Canada, Geomorphology, 95(1), 84–102, 2008.

Lantz, T. C. and S. V. Kokelj, S.V.: Increasing rates of retrogressive thaw slump activity in the Mackenzie Delta region, N.W.T., Canada, Geophys. Res. Lett., 35, L06502, doi:10.1029/2007GL032433, 2008.

Lantz, T.C., Kokelj, S. V., Gergel, S.E. and G.H.R. Henry: Relative impacts of disturbance and temperature: persistent changes in microenvironment and vegetation in retrogressive thaw slumps, Glob. Chang. Biol., 15(7), 1664–1675, doi:10.1111/j.1365-2486.2009.01917.x, 2009.

Lee, H., Schuur, E. A. G., Inglett, K. S., Lavoie, M. and Chanton, J. P.: The rate of permafrost carbon release under aerobic and anaerobic conditions and its potential effects on climate, Glob. Chang. Biol., 18, 515–527, doi:10.1111/j.1365-2486.2011.02519.x, 2012.

Lewkowicz, A. and Harris, C.: Morphology and geotechnique of active-layer detachment failures in discontinuous and continuous permafrost, northern Canada, Geomorphology, 69(1-4), 275–297, doi:10.1002/ppp.522, 2005.

Lewkowicz, A. G.: Morphology, frequency and magnitude of active-layer detachment slides, Fosheim Peninsula, Ellesmere Island, N.W.T., Nordicana, 54, 111–118, 1990.

Lewkowicz, A. G. and Harris, C.: Frequency and magnitude of active-layer detachment failures in discontinuous and continuous permafrost, northern Canada, Permafr. Periglac. Process., 16(1), 115–130, 2005.

746 Lovett, G.M., Cole, J.J., Pace, M.L.: Is net ecosystem production equal to ecosystem
747 carbon accumulation? Ecosystems, 9, 152–155, 2006.
748
749 Lund, M., Falk, J. M., Friborg, T., Mbufong, H. N., Sigsgaard, C., Soegaard, H. and
750 Tamstorf, M. P.: Trends in CO2 exchange in a high Arctic tundra heath, 2000-2010, J.
751 Geophys. Res. Biogeosciences, 117, G02001, doi:10.1029/2011JG001901, 2012.
752
753 Mackay, J.: Disturbances to the tundra and forest tundra environment of the western
754 Arctic, Can. Geotech. J.,7, 420-432, 1970.
755
756 Mauder, M. and Foken, T.: Documentation and Instruction Manual of the Eddy
757 Covariance Software Package TK2, Arbeitsergebn., Univ. Bayreuth, Abt. Mikrometeorol,
758 Bayreuth, Germany, 2004.
759
760 Mbufong, H. N., M. Lund, M. Aurela, T. R. Christensen, W. Eugster, T. Friborg, B. U.
761 Hansen, E. R. Humphreys, M. Jackowicz-Korczynski, L. Kutzbach, P. M. Lafleur, W. C.
762 Oechel, F. J. W. Parmentier, D. P. Rasse, A. V. Rocha, T. Sachs, M. M. van der Molen,
763 and M. P. Tamstorf (2014) Assessing the spatial variability in peak season CO2 exchange
764 characteristics across the Arctic tundra using a light response curve parameterization.
765 Biogeosciences 11, 4897–4912.
766
767 McGuire, A. D., Chapin, F. S., Walsh, J. E. and Wirth, C.: Integrated Regional Changes
768 in Arctic Climate Feedbacks: Implications for the Global Climate System *, Annu. Rev.
769 Environ. Resour., 31(1), 61–91, doi:10.1146/annurev.energy.31.020105.100253, 2006.
770
771 Merbold, L., Kutsch, W. L., Corradi, C., Kolle, O., Rebmann, C., Stoy, P. C., Zimov, S.
772 A. and Schulze, E. D.: Artificial drainage and associated carbon fluxes (CO2/CH4) in a
773 tundra ecosystem, Glob. Chang. Biol., 15(11), 2599–2614, 2009.
774
775 Nordstroem, C., Soegaard, H., Christensen, T. R., Friborg, T. and Hansen, B. U.:
776 Seasonal carbon dioxide balance and respiration of a high-arctic fen ecosystem in NE-
777 Greenland, Theor. Appl. Climatol., 70, 149–166, doi:10.1007/s007040170012, 2001.
778
779 Oberbauer, S. F., Tweedie, C. E., Welker, J. M., Fahnestock, J. T., Henry, G. H. R.,
780 Webber, P. J., Hollister, R. D., Walker, M. D., Kuchy, A., Elmore, E. and Starr, G.:
781 Tundra CO2 fluxes in response to experimental warming across latitudinal and moisture
782 gradients, Ecol. Monogr., 77(2), 221–238, 2007.
783
784 Paul-Limoges, E., Christen, A., Coops, N. C., Black, T. A. and Trofymow, J. A.:
785 Estimation of aerodynamic roughness of a harvested Douglas-fir forest using airborne
786 LiDAR, Remote Sens. Environ., 136, 225–233, doi:10.1016/j.rse.2013.05.007, 2013.
787
788 Pérez-Priego O, Serrano-Ortiz P, Sánchez-Cañete EP, Domingo F, Kowalski AS (2013)
789 Isolating the effect of subterranean ventilation on CO_2 emissions from drylands to the
790 atmosphere. Agric. For. Meteorol., 180, 194–202, 2013.
791

Rennermalm, A. K., Soegaard, H. and Nordstroem, C.: Interannual Variability in Carbon Dioxide Exchange from a High Arctic Fen Estimated by Measurements and Modeling, Arctic, Antarct. Alp. Res., 37, 545–556, doi:10.1657/1523-0430(2005)037[0545:IVICDE]2.0.CO;2, 2005.

Robinson, S.: Thaw-slump-derived thermokarst near Hot Weather Creek, Ellesmere Island, Nunavut, Geol. Surv. Canada Bull., 529, 335–345, 2000.

Robinson, S. D. and Pollard, W. H.: Massive ground ice within Eureka Sound bedrock, in Permafrost, Proc. 7th International Conf. on Permafrost, Yellowknife, Canada, Collection Nordicana, 23-27 June, 1998, 949–954, 1998.

Schuur, E. A. G., McGuire, A. D., Grosse, G., Harden, J. W., Hayes, D. J., Hugelius, G., Koven, C. D. and Kuhry, P.: Climate change and the permafrost carbon feedback, Nature, 520, 171–179, doi:10.1038/nature14338, 2015.

Schuur, E. A. G., Bockheim, J., Canadell, J. G., Euskirchen, E., Field, C. B., Goryachkin, S. V, Hagemann, S., Kuhry, P., Lafleur, P. M., Lee, H., Mazhitova, G., Nelson, F.E., Rinke, A., Romanovsky, V.E., Shiklomanov, N., Tarnocai, C., Venetsky, S., Vogel, J.G., and Zimov, S.A.: Vulnerability of permafrost carbon to climate change: Implications for the global carbon cycle, Bioscience, 58(8), 701–714, 2008.

Starr, G. and Oberbauer, S. F.: Photosynthesis of arctic evergreens under snow: Implications for tundra ecosystem carbon balance, Ecology, 84, 1415–1420, doi:10.1890/02-3154, 2003.

Stoy, P., Williams, M., Evans, J., Prieto-Blanco, A., Disney, M., Hill, T., Ward, H., Wade, T. and Street, L.: Upscaling tundra CO_2 exchange from chamber to eddy covariance tower, Arctic, Antarct. Alp. Res., 45, 275–284, doi:10.1657/1938-4246-45.2.275, 2013.

Tarnocai, C., Canadell, J. G., Schuur, E. A. G., Kuhry, P., Mazhitova, G. and Zimov, S.: Soil organic carbon pools in the northern circumpolar permafrost region, Global Biogeochem. Cycles, 23, GB2023, doi:10.1029/2008GB003327, 2009.

Ukraintseva, N.: Vegetation response to landslide spreading and climate change in the west Siberian tundra, in Proc. 9th International Conf. on Permafrost, Fairbanks, Alaska, 28 June – 3 July 2008, 2, 1793–1798., 2008.

Vincent, W., Callaghan, T., Dahl-Jensen, D., Johansson, M., Kovacs, K., Michel, C., Prowse, T., Reist, J. and Sharp, M.: Ecological implications of changes in the Arctic cryosphere, Ambio, 40, 87-99, doi:10.1007/s13280-011-0218-5, 2011.

Vogel, J., Schuur, E. A. G., Trucco, C. and Lee, H.: Response of CO_2 exchange in a tussock tundra ecosystem to permafrost thaw and thermokarst development, J. Geophys. Res. Biogeosciences, 114, G04018, doi:10.1029/2008JG000901, 2009.

838

839 Walter Anthony, K. M., Anthony, P., Grosse, G. and Chanton, J.: Geologic methane
840 seeps along boundaries of Arctic permafrost thaw and melting glaciers, Nat. Geosci., 5,
841 419–426, doi:10.1038/ngeo1480, 2012.

842

843 Wang, T., Ciais, P., Piao, S. L., Ottlé, C., Brender, P., Maignan, F., Arain, A., Cescatti,
844 A., Gianelle, D., Gough, C., Gu, L., Lafleur, P., Laurila, T., Marcolla, B., Margolis, H.,
845 Montagnani, L., Moors, E., Saigusa, N., Vesala, T., Wohlfahrt, G., Koven, C., Black, A.,
846 Dellwik, E., Don, A., Hollinger, D., Knohl, A., Monson, R., Munger, J., Suyker, A.,
847 Varlagin, A. and Verma, S.: Controls on winter ecosystem respiration in temperate and
848 boreal ecosystems, Biogeosciences, 8, 2009–2025, doi:10.5194/bg-8-2009-2011, 2011.

849

850 Welker, J. M., Fahnestock, J. T. and Jones, M. H.: Annual CO_2 flux in dry and moist
851 arctic tundra: Field responses to increases in summer temperatures and winter snow
852 depth, Clim. Change, 44, 139–150, doi:10.1023/a:1005555012742, 2000.

853

854 Welker, J. M., Fahnestock, J. T., Henry, G. H. R., O'Dea, K. W. and Chimner, R. A.:
855 CO_2 exchange in three Canadian High Arctic ecosystems: Response to long-term
856 experimental warming, Glob. Chang. Biol., 10(12), 1981–1995, 2004.
857
858
859
860
861
862
863
864
865
866
867
868
869
870
871
872
873
874
875
876
877
878
879
880
881
882
883

Tables

Table 1: Summary of net ecosystem exchange (*NEE*), soil temperatures (Soil T) and soil moisture (Soil M) from disturbed (d) and undisturbed (c) tundra, and air temperature (measured at T2) throughout the growing season.

Variable	Early Season	Peak Season	End Season
DOY	175-185	186-202	203-210
NEE_c (µmol m^{-2} s^{-1})*	0.080 ± 0.03	-0.28 ± 0.03	-0.015 ± 0.05
NEE_d (µmol m^{-2} s^{-1})*	0.55 ± 0.03	0.25 ± 0.03	0.58 ±0.13
Air Temperature (°C)			
mean (±SE)	10.5 ± 0.17	12.2 ± 0.10	7.2 ± 0.22
min/max	5.3 / 15.0	6.9 /16.1	2.0 / 12.0
Soil T_c (°C)* at 5 cm			
mean (±SE)	11.6 ± 0.05	11.9 ± 0.29	8.1 ± 0.05
min/max	5.4/ 19.8	6.9/19.8	2.6 / 16.2
Soil T_d (°C)* at 5 cm			
mean (±SE)	12.6 ± 0.07	11.9 ± 0.04	7.8 ± 0.07
min/max	6.6 / 19.1	6.8 / 19.5	2.1/ 15.2
Soil M_c (%)*			
mean (±SE)	14.4 ± 0.5	12.9 ± 0.4	16.9 ± 1.0
min/max	3.4 / 28.4	1.1 / 31.6	0.6 / 34.2
Soil M_d (%)*			
mean (±SE)	20.5 ± 0.8	24.8 ± 1.0	30.5 ± 1.6
min/max	9.7 / 41.2	4.1 / 45.4	6.9 / 44.8

* NEE_c = average net CO_2 flux from undisturbed (control) tundra.
* NEE_d = average net CO_2 flux from disturbed tundra.
* Soil T_c = average soil temperature from undisturbed tundra
* Soil T_d = average soil temperature from disturbed tundra
*Soil M_c = average soil temperature from undisturbed tundra
*Soil M_d = average soil temperature from disturbed tundra

902   Table 2: Summary of measurements (mean ± SE) from the portable chamber system (in

903   μmol m^{-2} s^{-1})

Variable	Location	Early	Peak	End	Total
DOY		175-185	186-202	203-210	
NEE	undisturbed	0.25 ± 0.10	-0.33 ± 0.15	-0.37 ± 0.15	-0.14 ± 0.13
	disturbed	0.31 ± 0.12	0.07 ± 0.13	0.11 ± 0.07	0.15 ± 0.06
GPP	undisturbed	0.85 ± 0.16	1.47 ± 0.26	1.00 ± 0.19	1.19 ± 0.19
	disturbed	0.39 ± 0.14	0.45 ± 0.16	0.24 ± 0.08	0.40 ± 0.03
R_e	undisturbed	1.10 ± 0.13	1.14 ± 0.15	0.62 ± 0.06	1.04 ± 0.12
	disturbed	0.70 ± 0.08	0.53 ± 0.10	0.35 ± 0.05	0.55 ± 0.06

904
905

906

907

908

909

910

911

912

913

914

915

916

Figures

Figure 1. Aerial image of the dual eddy covariance system setup with the location of both flux towers indicated. The valley trends NNE-SSW. View is to the south.

Figure 2. Turbulent source areas for two time-steps on DOY 186: a) 09:00 and b) 18:00, with ellipses displaying areas contributing to the given percentage of the signal from each instrument tower (T1 and T2). Three ellipses from each tower represent the 50%, 80%, and 90% cumulative source area. The shaded area represents a signal from the disturbed part of the surface. The white polygon represents the furthest extent of headwall retreat, as the initial image was taken in July 2013 (Worldview-2) and significant retreat occurred between image acquisition and the summer 2014 sampling period.

Figure 3. Meteorological conditions during the 2014 growing season at T2. Height of all instrumentation on the tower was 1 m above the canopy. Soil temperatures were measured at a depth of -5 cm, and mean temperature is shown for the disturbance (dashed line; n=7) and undisturbed tundra (solid line; n=14). DOY = day of the year.

Figure 4. Ensemble average diurnal course of soil temperatures in the disturbed and undisturbed sites throughout the season: Early season = 24 June – 4 July; Peak season = 5 July – 21 July; End of season = 22 July – 29 July. Boxes show the 25th and 75th percentiles, dots are the outliers, horizontal lines are medians.

Figure 5. Ensemble diurnal course of CO_2 fluxes from the retrogressive thaw slump (disturbed) and undisturbed tundra separated into the three sampling periods: top (early season), middle (peak season) and bottom (end season). Boxes show the 25th and 75th percentiles, black circles are outliers, horizontal lines are medians.

Figure 6. Average daily net CO_2 flux for the three sampling periods as measured by the two EC systems and the net effect for the entire season.

Figure 7. Comparison of NEE measurements from static chamber (square) and calculated from the two EC (circle) systems. Open symbols represent measurements from undisturbed tundra while closed symbols are measurements in the disturbed areas. Measurements were made in 21 collars in each of the disturbed and both undisturbed footprint areas of the EC towers.

Figure 8. Partitioning of NEE data from static chamber measurements into component fluxes, GPP and R_e for the undisturbed and disturbed sites. Measurements were made in 21 collars in each of the disturbed and both undisturbed footprint areas of the EC towers.